

3D VISION SYSTEM FOR THE RECOGNITION OF FREE PARKING SITE LOCATION

H. G. JUNG^{1)*}, D. S. KIM¹⁾, P. J. YOON¹⁾ and J. H. KIM²⁾

¹⁾Mando Central R&D Center, 413-5 Gomae-dong, Giheung-gu, Yongin-si, Gyeonggi 449-901, Korea

²⁾School of Electrical and Electronic Engineering, Yonsei University, Seoul 120-749, Korea

(Received 14 October 2005; Revised 24 February 2006)

ABSTRACT—This paper describes a novel stereo vision based localization of free parking site, which recognizes the target position of automatic parking system. Pixel structure classification and feature based stereo matching extract the 3D information of parking site in real time. The pixel structure represents intensity configuration around a pixel and the feature based stereo matching uses step-by-step investigation strategy to reduce computational load. This paper considers only parking site divided by marking, which is generally drawn according to relevant standards. Parking site marking is separated by plane surface constraint and is transformed into bird's eye view, on which template matching is performed to determine the location of parking site. Obstacle depth map, which is generated from the disparity of adjacent vehicles, can be used as the guideline of template matching by limiting search range and orientation. Proposed method using both the obstacle depth map and the bird's eye view of parking site marking increases operation speed and robustness to visual noise by effectively limiting search range.

KEY WORDS : Automatic parking system, Parking site marking, Stereo vision, Template matching

1. INTRODUCTION

Semi-automatic or full automatic parking system is one of the most interested driver assistant systems. Generally novice, female and old driver feels constraint in parking backward between vehicles. J. D. Power's 2001 Emerging Technology Study, which found that 66% of consumers were likely to purchase parking aid, is a good proof (Frank, 2004). Many upper class cars adopt ultrasonic parking assist system, which warns the driver of close distance to obstacle. Recently, car and component manufacturers started to provide vision based parking assist system. Toyota and Aisin Seiki introduced Back Guide Monitor, which helps the driver by projecting the predicted driving course on the image of a rear view camera (Furutani, 2004; Hiramatsu *et al.*, 2002). Aisin Seiki's next generation is expected to include circumstance recognition function to provide an optimistic view to the driver (Fintzel *et al.*, 2003). They use wheel speed sensor, structure from motion technology and virtual camera, i.e. IVR (Intermediate View Reconstruction) technology, to make a virtual rendered image from an optimistic viewpoint.

Automatic parking system automates parking operation

with automatic steering control and automatic braking control. Automatic parking system consists of three components: path planning including the localization of target position, automatic steering and braking system used to implement the planned trajectory, HMI (Human Machine Interface) used to receive the driver's input and provide the visual information of ongoing parking process. The localization of target position can be implemented by various methods, e.g. fully manual designation (Furutani, 2004), GPS infrastructure (Wada *et al.*, 2003) and the vision based localization of free parking site (Kaempchen *et al.*, 2002; Xu *et al.*, 2000). Toyota's IPA (Intelligent Parking Assist) is a semiautomatic parking system, which leaves the braking control as the driver's responsibility. Toyota's IPA developed the localization of target position by HMI, which shows a potential target position on the image of a rear view camera and enables the driver to change the target position with direction control buttons such as up, down, left, right and rotation (Furutani, 2004).

Although semiautomatic parking system becomes commercialized, fully manual designation is too tedious and complicated for daily usage. Therefore, it is natural that the need of the vision based localization of free parking site is increasing rapidly. Nico Kaempchen developed stereo vision based pose estimation of parking lots, which uses feature based stereo algorithm, template

*Corresponding author. e-mail: hgjung@mando.com

matching algorithm on a depth map and 3D fitting to the planar surface model of vehicle by ICP (Iterative Closest Point) algorithm (Kaempchen *et al.*, 2002). The vision system uses the disparity of vehicles but ignores all the information of parking site marking. Jin Xu developed color vision based localization of parking site marking, which uses color segmentation based on RCE neural network, contour extraction based on least square method and inverse perspective transformation (Xu *et al.*, 2000). Because the system depends only on parking site marking, it can be degraded by poor visual conditions such as stain on marking, shadow and occlusion by adjacent vehicles.

This paper proposes a novel vision system to localize free parking site for automatic parking system. Proposed method is based on feature based stereo matching and separates parking site marking by plane surface constraint. The location of parking site is determined by template matching on the bird's eye view of parking site marking, which is generated by the inverse perspective transformation on the separated parking site marking. Obstacle depth map, which is generated by the disparity information of adjacent vehicles, can be used to narrow the search range of parking site center and the orientation. Because the template matching is fulfilled within a limited range, the speed of searching effectively increases and the result of searching is robust to the noise including previously mentioned poor visual conditions. Using both obstacle depth map and parking site marking can be justified because typical parking site in urban area is constructed by nation-wide standards.

2. SYSTEM CONFIGURATION

Figure 1 shows the configuration of semi-automatic parking system used for the experiments. R-EPS (Rack type Electric Power Steering) is used as an active steering system, which fulfils steering angle command sent from parking controller. Stereo vision camera is off-the-shelf product and installed at the back-end of test vehicle using protection case like Figure 2(a). Driver interface, i.e. HMI, is implemented with touch screen monitor like Figure 2(b). Through the driver interface, system informs the progress of ongoing parking operation and shows the backward view. At the end of automatic parking, EPB (Electric Parking Brake) is activated to finish the parking operation.

In semi-automatic parking system, ultimate responsibility remains to driver. Driver must pay attention to surrounding situation and controls the parking operation by manual brake handling. Therefore, semi-automatic parking system is different from full automatic parking system not only in the viewpoint of automatic braking but also in the viewpoint of surrounding monitoring.

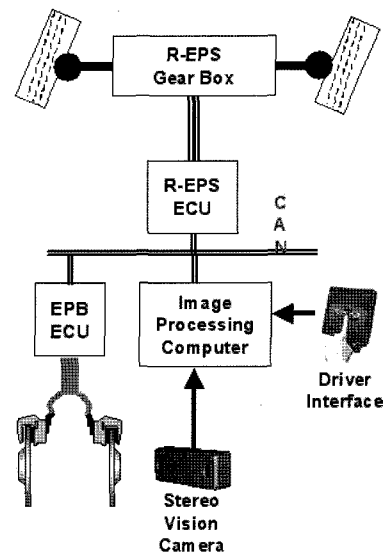


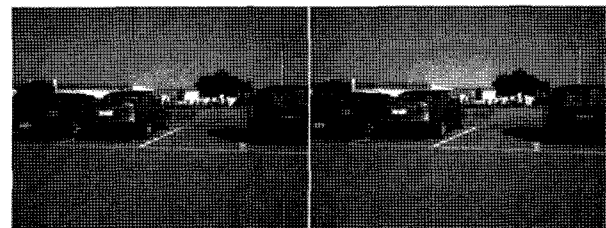
Figure 1. Semi-automatic parking system.



(a) Camera installation

(b) HMI

Figure 2. Test vehicle.



(a) Left image

(b) Right image

Figure 3. Stereo image.

3. STEREO VISION SYSTEM

Figure 3 is the stereo image of typical parking site, which is acquired with Point Grey Research's Bumblebee camera installed on the backend of test vehicle. Each image has 640×480 resolution and 24 bits color information. The images are rectified with Point Grey Research's Triclops rectification library (Point Grey Research, 2005). In Figure 3, it is observed that some portion of parking site marking is occluded by adjacent vehicle and trash. Some portion of parking site marking is invisible because of shadow.

3.1. Pixel Classification

4 neighbors

	0	
3	X	1
	2	

$$d(i) = \begin{cases} 1, & \text{if } g(i)-g(x) > +T \\ 2, & \text{if } g(i)-g(x) < -T \\ 0, & \text{else} \end{cases} \quad (1)$$

$g(\cdot)$: grey value

Pixel Class	d(3)	d(2)	d(1)	d(0)
-------------	------	------	------	------

In the case of automotive vision, it is known that vertical edges are sufficient to detect noticeable objects (Gavrila *et al.*, 2001). Consequently, stereo matching using only the vertical edges drastically reduces the computational load (Franke and Joos, 2000; Franke and Kutzbach, 1996). Pixel classification investigates the intensity differences between a pixel and 4 directly connected neighbors so as to assign the pixel a class reflecting the intensity configuration. It is known that the feature based stereo matching with pixel class is fast and robust to noise (Franke and Kutzbach, 1996). Equation (1) shows that a pixel of smooth surface will be classified as zero class and a pixel of edge will be classified as non-zero class. To reduce the effect of threshold T, histogram equalization or adaptive threshold can be used.

Figure 4 shows the result of the pixel classification. 13.7% of total pixels are classified as horizontal edge and 7.8% are classified as vertical edge.

3.2. Feature Based Stereo Matching

Stereo matching is performed only on pixels classified as vertical edge. Furthermore, stereo matching is composed of step-by-step test sequences through class comparison, class similarity, color similarity and maximum similarity detection. Only correspondence candidates passing the previous test step will be investigated in the next test step.

$$\text{ClassSimilarity}(x,y,s) = \frac{1}{3 \times 3} \sum_{u=-1}^1 \sum_{v=-1}^1 f(\text{Class}_{\text{left}}(x+u,y+v), \text{Class}_{\text{right}}(x+u+s,y+v)) \quad (2)$$

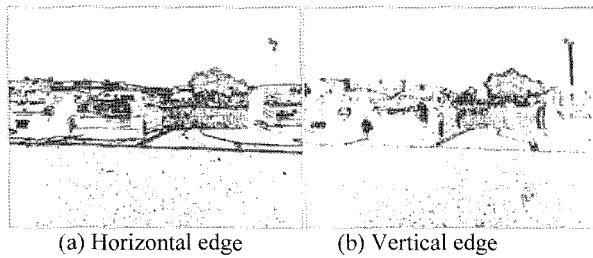
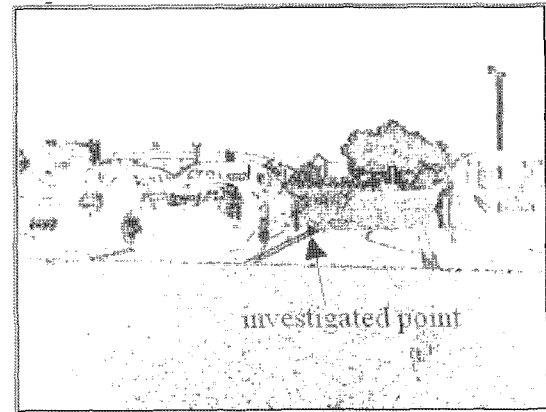
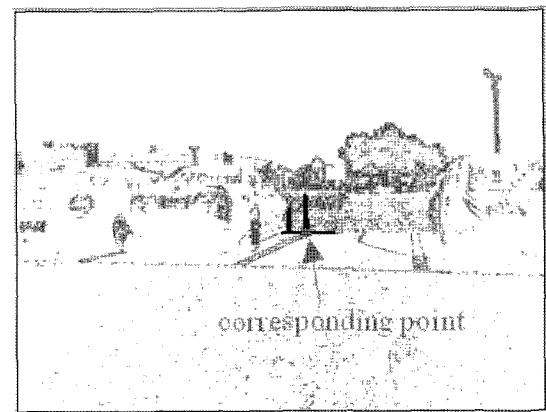


Figure 4. Pixel classification result.



(a) Left image



(b) Right image

Figure 5. Stereo matching result.

$$\text{where } f(\text{Class}_{\text{left}}, \text{Class}_{\text{right}}) = \begin{cases} 0, & \text{Class}_{\text{left}} \neq \text{Class}_{\text{right}} \\ 1, & \text{Class}_{\text{left}} = \text{Class}_{\text{right}} \end{cases}$$

$$\text{ColorSimilarity}(x,y,s) = 1 - \frac{1}{256} \sqrt{\frac{\text{ColorSSD}(x,y,s)}{5 \times 5}} \quad (3)$$

$$\text{where ColorSSD}(x,y,s) = \sum_{u=-2}^2 \sum_{v=-2}^2 \left\{ \begin{aligned} &(\text{R}_{\text{left}}(x+u,y+v) - \text{R}_{\text{right}}(x+u+s,y+v))^2 + \\ &(\text{G}_{\text{left}}(x+u,y+v) - \text{G}_{\text{right}}(x+u+s,y+v))^2 + \\ &(\text{B}_{\text{left}}(x+u,y+v) - \text{B}_{\text{right}}(x+u+s,y+v))^2 \end{aligned} \right.$$

$$\text{Similarity}(x,y,s) = \text{ClassSimilarity}(x,y,s) \times \text{ColorSimilarity}(x,y,s) \quad (4)$$

Assuming that the vertical alignment of Bumblebee is correct, the search range of a pixel is limited to a horizontal line with $-35 \sim 35$ displacement. First, correspondence test is performed on pixels with the same class as the investigated pixel. Class similarity defined by equation (2) is the measure of how the candidate pixel is similar to the investigated pixel in the sense of 3×3 class window. Color similarity defined by equation (3) is the measure of

how the candidate pixel is similar to the investigated pixel in the sense of 5×5 color window. Total similarity defined by equation (4) is the product of the class similarity and the color similarity. If highest total similarity is lower than a certain threshold, the investigated pixel fails to find corresponding point and is ignored.

Figure 5 shows the stereo matching result of a pixel. Graph on right image is the total similarity of pixels within search range. The pixel with highest total similarity is corresponding point.

3.3. Road/Object Separation

Generally, pixels on the road surface satisfy plane surface constraint, i.e. the y coordinate of a pixel is in linear relationship with the disparity of the pixel, $d(x,y)$, like equation (5) (Franke and Kutzbach, 1996). Consecutively, the pixels of obstacles, e.g. adjacent vehicles, do not follow the constraint. Therefore, the disparity map which is the result of stereo matching can be separated into two disparity maps: the disparity map of parking site marking and the disparity map of obstacle.

$$d(x,y) = \frac{B}{H} f_x \left(\frac{y}{f_y} \cos \alpha + \sin \alpha \right), \quad \text{with } y > f_y \tan \alpha \quad (5)$$

where B: baseline, H: Height,
 f_x, f_y : focal length, α : tilt angle

$$Z_{\text{world}} = \frac{B \cdot f}{d(x,y)} \quad (6-1)$$

$$d(x,y) = P_1 y + P_2 \quad (6-2)$$

where $P_1 = \frac{B f_x}{H f_y} \cos \alpha$, $P_2 = \frac{B f_x}{H f_y} \sin \alpha$

$$Z_{\text{world}} = \frac{B \cdot f}{P_1 \cdot y + P_2} \quad (6-3)$$

$$y = \frac{1}{P_1} \left(\frac{B \cdot f}{Z_{\text{world}}} - P_2 \right) \quad (6-4)$$

$$X_{\text{world}} : Z_{\text{world}} = x : f \Rightarrow x = \frac{f \cdot X_{\text{world}}}{Z_{\text{world}}} \quad (6-5)$$

The distance between camera and object, Z_{world} , is

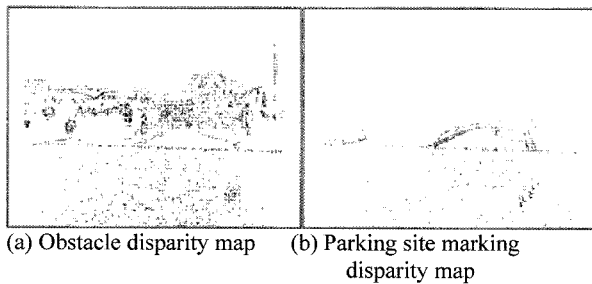


Figure 6. Road/object separation result.

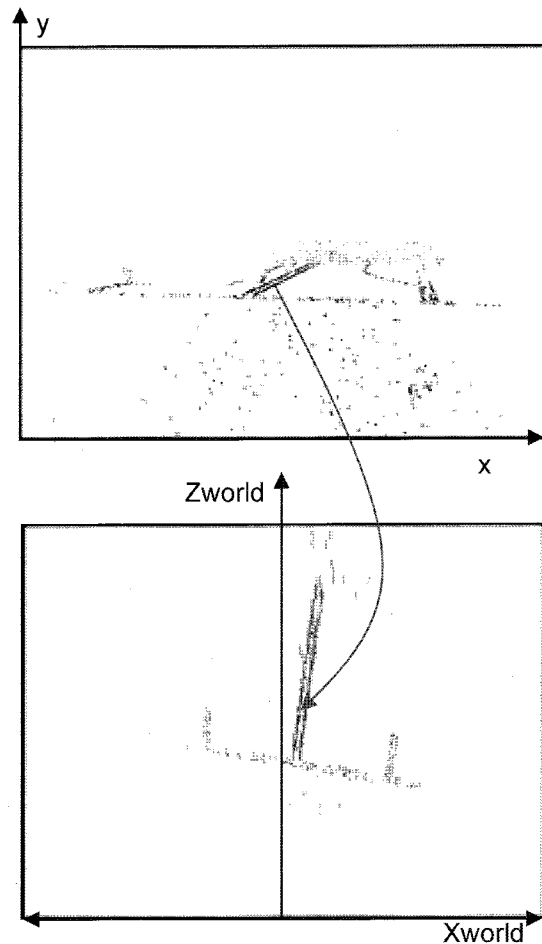


Figure 7. Bird's eye view of parking site marking.

inverse proportional to the disparity like equation (6-1). Previously mentioned plane surface constraint can be simplified like equation (6-2). P_1 and P_2 is the constant parameter of camera configuration. Consequently, the relationship between the y coordinate of a pixel on road surface and Z_{world} can be summarized like equation (6-3), (6-4). The relationship between X_{world} and the x coordinate of a pixel can be defined like (6-5) by triangulation. Using the relationship, the disparity map of parking site marking is transformed into the bird's eye view of parking site marking. The bird's eye view is constructed by copying values from the disparity map to the ROI (Region Of Interest) of X_{world} and Z_{world} . Pixels with different color from parking site marking are ignored to remove the noise of textures such as asphalt and grass.

Obstacle depth map is constructed by projecting the disparity information of pixels unsatisfying the plane surface constraint. World coordinate point ($X_{\text{world}}, Z_{\text{world}}$) corresponding to a pixel in the obstacle disparity map can be determined by equation (6-1) and (6-5) (Franke and Joss, 2000). Because the stereo matching does not

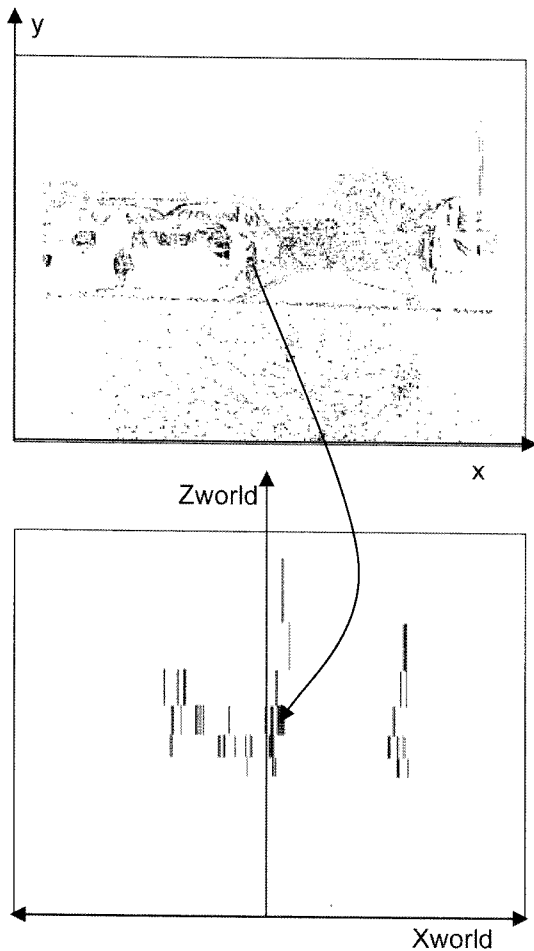


Figure 8. Obstacle depth map.

implement sub-pixel resolution for real time performance, a pixel in the disparity map contributes to a vertical array in the depth map. The element of depth map accumulates the contributions of corresponding disparity map pixels. By eliminating the elements of depth map under a certain threshold, noise on the disparity map can be removed. In general, the noise of the disparity map does not make a peak on the depth map.

4. LOCALIZATION OF PARKING SITE

Free parking site is localized using both the depth map of obstacle and the bird's eye view of parking site marking. Localization algorithm consists of 3 steps: finding guideline, obstacle histogram and template matching.

Guideline, which is the front line of parking area, is found by the Hough transform of the bird's eye view of parking site marking. The pose of ego-vehicle is limited to $-40\sim 40$ degrees with respect to the longitudinal direction of parking area. Therefore, the peak of Hough transform in this angular range is the guideline as depicted in

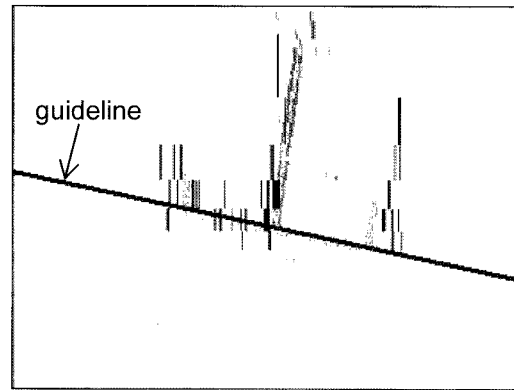


Figure 9. Recognized guideline.

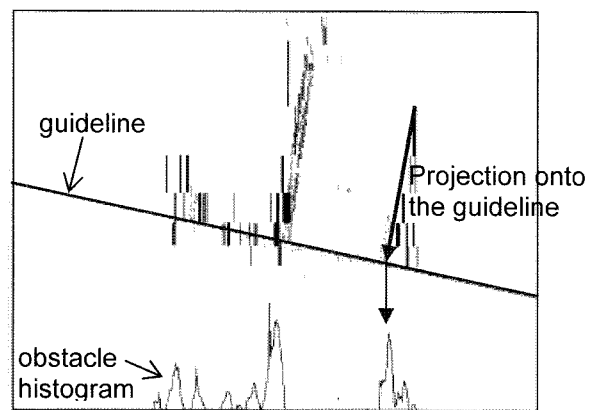
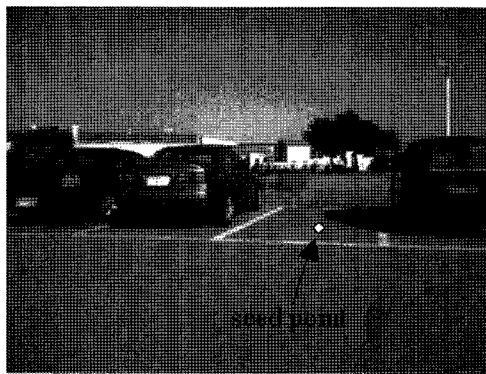


Figure 10. Obstacle histogram.

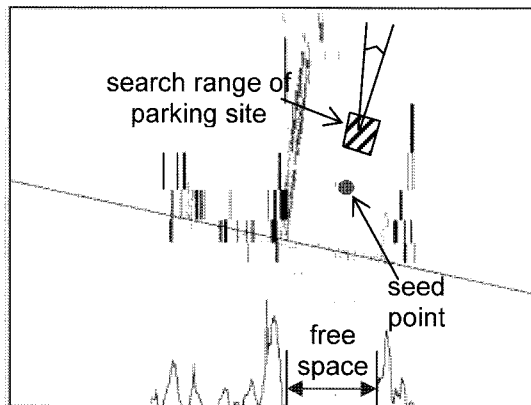
Figure 9.

Obstacle histogram determines the free range of the guideline. Adjacent vehicles are expected to be located in the direction orthogonal to the guideline because parking area is divided in such a way. Therefore, accumulating the occurrence of meaningful depth map points in that direction can separate occupied parking site from free parking site. Obstacle histogram is implemented as an integer array having the same size as the length of guideline. Inner product between the guideline vector and the meaningful depth map point vector produces a scalar value, which is used as the index of histogram array. Then, array element designated by the index increases. Figure 10 shows the resultant obstacle histogram. It can be observed that free parking site has very low value in the obstacle histogram.

Free space is the continuous portion of the obstacle histogram under a certain threshold and is determined by bidirectional search from the seed point. The search range of parking site center in the guideline direction is central 20% of the free space. The initial guess of parking site center in another direction, i.e. orthogonal to guideline direction, is the position distant from the guideline by



(a) Seed point designated by driver



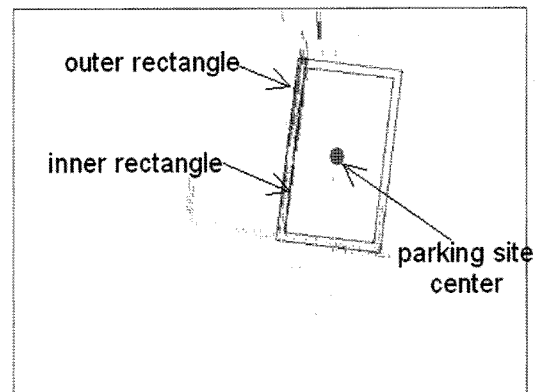
(b) Search range of parking site center

Figure 11. Seed point and search range.

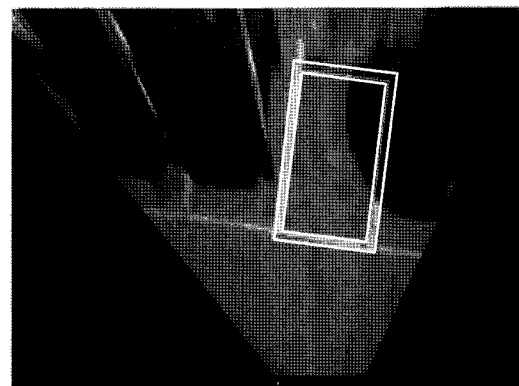
the half size of template length. The search range in the orthogonal direction is 10 pixels and the angular search range is 10 degrees.

If one of side parking sites is not occupied, free space will be too long compared with the width of parking site template. In this case, free space is modified to a range having the same length as the width of parking site template from the detected obstacle.

Final template matching uses a template consisting of 2 rectangles derived from the standards about parking site drawing. The template matching measures how many pixels of parking site marking exist between 2 rectangles, i.e. between inner and outer rectangle. Figure 12(a) shows the result on the bird's eye view of parking site marking and Figure 12(b) projects the result on the bird's eye view of input image. Because the search range is narrowed by the obstacle depth map, template matching successfully detects the correct position in spite of stain, blurring and shadow. Furthermore, template matching, which is the bottleneck of localization process, consumes little time. Total computational time on 1 GHz PC is about 400–500 msec. Once the initial position is detected successfully, the next scene needs only template match-



(a) Result on parking site marking



(b) Result on input image

Figure 12. Detected parking site.

ing with little variation around the previous result.

5. CONCLUSION

This paper proposes a stereo vision based 3D localization of the target position of automatic parking system. Pixel classification and feature based stereo matching produces disparity map in real time. Road and object are separated by plane surface constraint, then transformed into bird's eye view and depth map respectively. Obstacle depth map establishes the search range of free parking site and simple template matching finds the exact location of free parking site. By using both parking site marking and obstacle depth map, the search range of template matching is drastically reduced and the result is robust to noise such as stain, waste and shadow. Hereafter, research on the variation of parking site marking is needed.

REFERENCES

- Fintzel, K., Bendahan, R., Vestri, C., Bougnoux, S., Yamamoto, S. and Kakinami, T. (2003). 3D vision system for vehicles. *Proc. IEEE Intelligent Vehicle*

- Symp.*, 174–179.
- Frank, R. (2004). Sensing in the ultimately safe vehicle. *SAE Paper No. 2004-21-0055*.
- Franke, U. and Joos, A. (2000). Real-time stereo vision for urban traffic scene understanding. *Proc. IEEE Intelligent Vehicle Symp.*, 273–278.
- Franke, U. and Kutzbach, I. (1996). Fast stereo based object detection for stop&go traffic. *Proc. IEEE Intelligent Vehicle Symp.*, 339–344.
- Furutani, M. (2004). Obstacle detection systems for vehicle safety. *SAE Paper No. 2004-21-0057*.
- Gavrila, D. M., Franke, U., Woehler, C. and Goerzig, S. (2001). Real-time vision for intelligent vehicles. *IEEE Instrumentation & Measurement Magazine* **4**, **2**, 22–27.
- Hiramatsu, S., Hibi, A., Tanake, Y., Kakinami, T., Iwata, Y. and Nakamura, M. (2002). Rearview camera based parking assist system with voice guidance. *SAE Paper No. 2002-01-0759*.
- Kaempchen, N., Franke, U. and Ott, R. (2002). Stereo vision based pose estimation of parking lots using 3D vehicle models. *Proc. IEEE Intelligent Vehicle Symp.*, 459–464.
- Point Grey Research (2005). *Point Grey Research's Homepage*, <http://www.ptgrey.com>.
- Wada, M., Yoon, K. S., Hashimoto, H. (2003). Development of advanced parking assistance system. *IEEE Trans. Industrial Electronics* **50**, **1**, 4–17.
- Xu, J., Chen, G. and Xie, M. (2000). Vision-guided automatic parking for smart car. *Proc. IEEE Intelligent Vehicle Symp.*, 725–730.